

ON OPTIMAL ANCHOR NODE PLACEMENT IN SENSOR LOCALIZATION BY OPTIMIZATION OF SUBSPACE PRINCIPAL ANGLES

Joshua N. Ash and Randolph L. Moses

Department of Electrical and Computer Engineering
Ohio State University, Columbus, OH 43210

ABSTRACT

In sensor network self-localization, anchor nodes provide a convenient means to disambiguate scene translation and rotation, thereby affording estimates in an absolute coordinate system. However, localization performance depends on the positions of the anchor nodes relative to the unknown-location nodes. Conventional wisdom in the literature is that anchor nodes should be placed around the perimeter of the network. In this paper, we show analytically why this strategy works well universally. We demonstrate that perimeter placement forces the information provided by the anchor constraints to closely align with the subspace that cannot be estimated from inter-node measurements: the subspace of translations and rotations. Examples quantify the efficacy of perimeter placement of anchors.

Index Terms— sensor network localization, anchor nodes, constrained estimation, principal angles, subspace alignment

1. INTRODUCTION

In the majority of sensor network applications, knowledge of the absolute sensor positions is necessary in order to obtain meaningful information from sensed data. Numerous localization algorithms have been proposed to establish sensor locations from inter-sensor measurements, such as distances, time-of-arrival, time-difference-of-arrival or received-signal-strength (see, e.g. [1], and references therein). These inter-sensor measurements are, however, invariant to translations and rotations of the sensor network; meaning that the measurements alone only provide information about the relative shape of the network—not its absolute location, as is needed in most environmental monitoring applications.

In order to regularize the absolute localization problem, additional information or assumptions are needed about the network. We could, for example, specify the location of the scene centroid and the angle from the centroid to one of the sensors. In a Bayesian setting, prior distributions on a subset of sensor positions can be used to regularize the problem [2]. As the variance of these priors goes to zero, this is equivalent to precisely specifying the location of a subset of the sensors. Known-location sensors are called anchor nodes (or beacon nodes), and they are commonly used in localization because of their relative ease of measurement. However, the performance of absolute localization is sensitive to the position of the anchor nodes relative to the remainder of unknown-location nodes.

Conventional wisdom in the localization literature is that anchor nodes should be uniformly spread around the perimeter of the network—observations made empirically by several researchers [3, 4, 5] for multiple algorithms and measurement types. In this paper

This work was supported in part by an MIT Lincoln Laboratory Graduate Fellowship of the first author.

we provide analytical justification that uniform perimeter placement is an optimal strategy in the absence of other information about the sensor locations.

2. BACKGROUND

2.1. Sensor localization

In anchor-based localization the positions $\theta_a = [x_1 \ y_1 \ \dots \ x_{n_a} \ y_{n_a}]$ of a set of n_a anchor nodes and set of measurements z are used to estimate the positions $\theta_u = [x_{n_a+1} \ y_{n_a+1} \ \dots \ x_n \ y_n]$ of $n_u = n - n_a$ unknown-location nodes. The measurements are inter-node measurements between the n sensors but need not contain all pairwise combinations. In the following it will be useful to consider the equivalent problem of estimating $\theta = [\theta_a, \theta_u]$ under a constraint on θ_a . In order to quantify localization performance, we consider the Cramér-Rao bound (CRB) for θ_u . Fisher's information matrix $J(\theta_a, \theta_u)$ for θ_u depends on the locations of the unknown-location sensors as well as the anchor locations, and it also depends on the type of inter-node measurements and the distribution of the measurement noise. If all of these quantities were known, we could find the CRB-optimal anchor locations as

$$\theta_a^* = \arg \min_{\theta_a} \text{tr} J^{-1}(\theta_u, \theta_a). \quad (1)$$

Alternatively, we consider an anchor placement strategy which does not depend on the sensor positions or the noise distributions. When the measurements z are invariant to global translations and rotations of the entire scene θ —as they are for distance and time-of-arrival measurements—we are not able to uniquely estimate θ without the anchors constraining a portion of the network. That is to say, there are an infinite number of scene configurations $\{\theta\}$ (all translations and rotations of one another) which are all equally likely of producing a given set of measurements z . The anchor nodes remove this ambiguity, and as such, in lieu of any additional information, should be positioned in such a way that this translational and rotational ambiguity is minimized in some sense.

2.2. Constraint and transformation subspaces

We may write the anchor constraint as

$$C_a^T \theta = \theta_a^0, \quad (2)$$

where $C_a^T = [I_{2n_a} \ 0] \in \{0, 1\}^{2n_a \times 2n}$ extracts the anchor coordinates from θ , and θ_a^0 are the constrained anchor positions. The components of θ in the range space $\mathcal{R}(C_a)$ are fully determined by the constraint. We call $\mathcal{C} = \mathcal{R}(C_a)$ the *constraint subspace*.

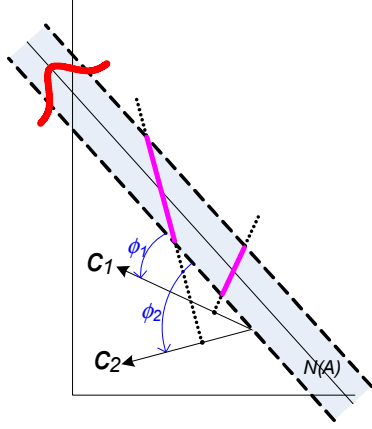


Fig. 1: Constraint alignment example. When the linear constraints are closely aligned with the non-measurable subspace, lower estimation error results. Here, constraint c_1 is closest to the nullspace $\mathcal{N}(A)$ and the resulting x -uncertainty is less than for constraint c_2 .

In [6], a linear approximation of the space of all translations and rotations of θ was given as the span of the three $2n$ -vectors

$$v_x = \frac{1}{c_1} \begin{bmatrix} 1 \\ 0 \\ 1 \\ 0 \\ \vdots \end{bmatrix}, v_y = \frac{1}{c_1} \begin{bmatrix} 0 \\ 1 \\ 0 \\ 1 \\ \vdots \end{bmatrix}, v_\phi = \frac{1}{c_2} \begin{bmatrix} -(y_1 - \bar{y}) \\ (x_1 - \bar{x}) \\ -(y_2 - \bar{y}) \\ (x_2 - \bar{x}) \\ \vdots \end{bmatrix}, \quad (3)$$

where v_x and v_y represent x and y translations, v_ϕ corresponds to rotation about the centroid (\bar{x}, \bar{y}) , and $c_1 = n^{\frac{1}{2}}$ and $c_2 = (\sum_{i=1}^n (x_i - \bar{x})^2 + (y_i - \bar{y})^2)^{\frac{1}{2}}$ are normalization constants. That is, $(\theta + \alpha_x v_x)$ and $(\theta + \alpha_y v_y)$ provide x - and y -translated versions of θ , while $(\theta + \alpha_\phi v_\phi)$ locally approximates a rigid rotation of θ . As such, we may say that the measurements do not provide any information about the components of θ in $\mathcal{V} = \mathcal{R}(V)$, where $V = [v_x \ v_y \ v_\phi]$. We call \mathcal{V} the *transformation subspace*.

Intuitively, it is desirable for the constraints to provide as much information as possible about the components of θ in the subspace \mathcal{V} which is not informed upon by measurements. Figure 1 illustrates an example of an under determined linear system where the measurements $y = Ax + e$ provide no information about the value of x in the nullspace $\mathcal{N}(A)$. The error term e establishes an uncertainty band about $\mathcal{N}(A)$. Two constraint vectors c_1, c_2 are considered with corresponding constraints $c_i^T x = h_i$, $i = 1, 2$, for scalars h_i . Specifying the value of x along the direction c_i constrains x to the subspace orthogonal to c_i and establishes a “cut” through the uncertainty ribbon. When the angle ϕ_i between c_i and $\mathcal{N}(A)$ is small, the resulting uncertainty in x is small. In the example, $\phi_1 < \phi_2$ and c_1 results in lower final uncertainty in x .

In general, when the constraint and uncertain subspaces have larger dimensions, there are many angles between the vectors $c \in \mathcal{C}$ and $v \in \mathcal{V}$. If any vector $v \in \mathcal{V}$ is orthogonal to all of \mathcal{C} then at least one component (direction) of θ remains completely unconstrained and unspecified by measurements. As a surrogate to the anchor optimization problem in Eq. (1) we consider the anchor locations which minimize the maximum angle between \mathcal{C} and \mathcal{V} . We will see in the following section that this strategy is independent of the unknown sensor locations θ_u .

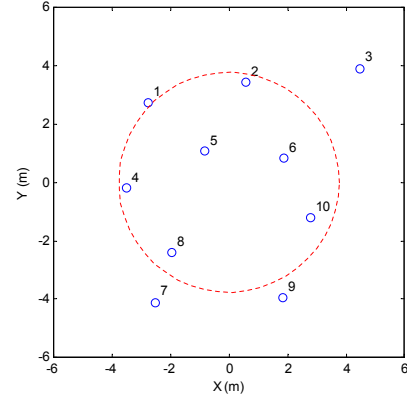


Fig. 2: Sample network with 10 unknown-location sensors. Examples will add additional anchor nodes to the scene in order to perform absolute localization. The circle indicates the RMS radius of the 10 sensors.

2.3. Principal angles

For reference, we summarize in this subsection the definition and some properties of principal angles between subspaces.

Let \mathcal{A} and \mathcal{B} be two subspaces of dimension d_a and d_b respectively, $d_b \geq d_a$. The principal angles $\phi_1, \dots, \phi_{d_a} \in [0, \pi/2]$ between \mathcal{A} and \mathcal{B} are defined recursively [7] as

$$\cos \phi_i = \max_{\substack{a \in \mathcal{A} \\ \|a\|=1}} \max_{\substack{b \in \mathcal{B} \\ \|b\|=1}} a^T b = a_i^T b_i \quad (4)$$

subject to

$$a^T b_j = 0 \quad j \in \{1, \dots, i-1\} \quad (5)$$

$$b^T a_j = 0 \quad j \in \{1, \dots, i-1\}. \quad (6)$$

The principal angles satisfy $0 \leq \phi_1 \leq \dots \leq \phi_{d_a} \leq \pi/2$ and ϕ_{d_a} is the largest angle between any vector in \mathcal{A} and any vector in \mathcal{B} not orthogonal to \mathcal{A} .

The principal angles may be computed as

$$\cos \phi_i = \sigma_i \quad i \in \{1, \dots, d_a\}, \quad (7)$$

where σ_i is the i^{th} largest singular value of $A^T B$, with orthonormal matrices A and B having column spans equal to \mathcal{A} and \mathcal{B} , respectively.

3. OPTIMAL ANCHOR POSITIONS

In this section we consider finding the anchor positions which are optimal in the sense that they minimize the angles between the constraint subspace \mathcal{C} and the unknown transformation space \mathcal{V} .

3.1. Derivation of principal angles

We assume, without loss of generality, that the centroid (\bar{x}, \bar{y}) is at the origin $(0, 0)$ and that the number of anchors $n_a \geq 3$ since this is sufficient to disambiguate translations, rotations, and mirror images. The dimension of \mathcal{V} is 3, so there are only 3 principal angles. The matrices V and C_a have orthonormal columns spanning \mathcal{V} and \mathcal{C} ;

and, we seek the singular values of the $3 \times 2n_a$ matrix $Q = V^T C_a$, or the eigenvalues of QQ^T . Here, Q is

$$Q = \begin{bmatrix} \frac{1}{c_1} & 0 & \frac{1}{c_1} & 0 & \dots & \frac{1}{c_1} & 0 \\ 0 & \frac{1}{c_1} & 0 & \frac{1}{c_1} & \dots & 0 & \frac{1}{c_1} \\ \frac{-y_1}{c_2} & \frac{x_1}{c_2} & \frac{-y_2}{c_2} & \frac{x_2}{c_2} & \dots & \frac{-y_{n_a}}{c_2} & \frac{x_{n_a}}{c_2} \end{bmatrix}, \quad (8)$$

and

$$QQ^T = \begin{bmatrix} q & 0 & a \\ 0 & q & b \\ a & b & c \end{bmatrix}, \quad (9)$$

where $q = \frac{n_a}{c_1^2}$, $a = \frac{-1}{c_1 c_2} \sum_{i=1}^{n_a} y_i$, $b = \frac{1}{c_1 c_2} \sum_{i=1}^{n_a} x_i$, and $c = \frac{1}{c_2^2} \sum_{i=1}^{n_a} (x_i^2 + y_i^2)$. The eigenvalues of QQ^T , in order from largest to smallest, are

$$\lambda_1 = \frac{1}{2}(c+q) + \frac{1}{2}\sqrt{(c-q)^2 + 4(a^2 + b^2)} \quad (10)$$

$$\lambda_2 = q \quad (11)$$

$$\lambda_3 = \frac{1}{2}(c+q) - \frac{1}{2}\sqrt{(c-q)^2 + 4(a^2 + b^2)}. \quad (12)$$

The principal angles are

$$\phi_i = \cos^{-1} \sqrt{\lambda_i} \quad i = 1, 2, 3. \quad (13)$$

3.2. Angular positioning of anchors

Equivalent to minimizing the maximum principal angle between C and \mathcal{V} , we maximize the minimum eigenvalue λ_3 . Observe that

$$a^2 + b^2 = \frac{(\bar{x}_a)^2 + (\bar{y}_a)^2}{(n/n_a^2) \|\theta\|^2}, \quad (14)$$

where \bar{x}_a is the average x -coordinate of the anchor nodes and \bar{y}_a is the average y -coordinate. With respect to a and b , λ_3 is maximized when $a^2 + b^2 = 0$, which occurs when the mean x and mean y coordinates of the anchors are zero. One configuration that achieves this is when all anchors are uniformly distributed around a circle of any radius.

With respect to c , λ_3 achieves its maximum value of q whenever $c \geq q$.

3.3. Radial positioning of anchors

The variable c may be written

$$c = \frac{\|\theta_a\|^2}{\|\theta_a\|^2 + \|\theta_u\|^2}. \quad (15)$$

Therefore, c may be made arbitrarily large by placing the anchors progressively farther from the scene center. When $c \geq q$, we have $\lambda_2 = \lambda_3 = n_a/n$ and $\lambda_1 = c$. Hence, having maximized the two smallest eigenvalues we could proceed to maximize λ_1 , the largest eigenvalue. λ_1 is maximized by maximizing $\|\theta_a\|$, which is achieved by pushing all of the anchor nodes as far out from the centroid as possible (given measurement and deployment constraints). However, because the smallest eigenvalue (largest principal angle) dominates performance, we expect negligible performance in extending λ_1 significantly beyond the other two eigenvalues $\lambda_2 = \lambda_3 = n_a/n$. Therefore, we attempt to equate all three eigenvalues.

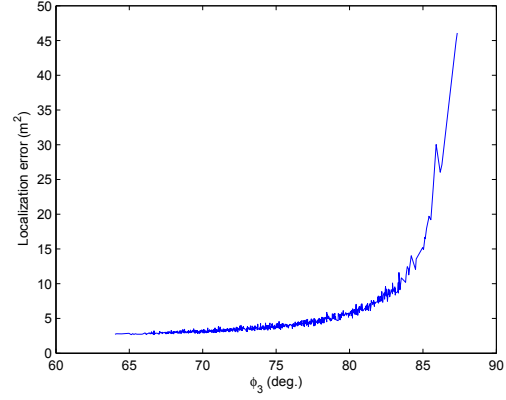


Fig. 3: Mean-square localization error versus maximum principal angle ϕ_3 for the network in Fig. 2 using 3 anchor nodes.

Setting $\lambda_1 = c = n_a/n$, we solve

$$\frac{\|\theta_a\|^2}{\|\theta_a\|^2 + \|\theta_u\|^2} = \frac{n_a}{n} \quad (16)$$

for $\|\theta_a\|^2$ and obtain

$$\|\theta_a\|^2 = \frac{n_a}{n - n_a} \|\theta_u\|^2. \quad (17)$$

If we assume that all n_a anchors have a common radius r_0 , then $\|\theta_a\|^2 = n_a r_0^2$. Substituting this and $n_u = n - n_a$ into (17) and solving for r_0 we find

$$r_0 = \frac{\|\theta_u\|}{\sqrt{n_u}}. \quad (18)$$

The quantity r_0 may be interpreted as the root-mean-square (RMS) distance of the unknown-location sensors from the origin. For the sample network in Figure 2, the RMS sensor radius r_0 is illustrated by the circle in the figure. When the anchors are all uniformly spaced around a circle of radius r_0 , all three principal angles will be equal to $\phi = \cos^{-1}(\sqrt{n_a/n})$. In practice, it is simpler to place the anchors around the sensor field perimeter which will always have a radius greater or equal to r_0 .

4. EXAMPLES

As in Eq. (1), we take as our performance metric the trace of the CRB. In these examples we assume that all sensors (unknown-location nodes and anchors) make pairwise distance measurements to one another and that the distance measurements are independently corrupted by zero-mean Gaussian noise with variance σ^2 . Fisher's information matrix (FIM) for the non-anchors may be written $J = 1/\sigma^2 J_1(\theta_u, \theta_a)$, where J_1 is the FIM corresponding to $\sigma = 1$. The mean-square error bound is $e = \text{tr } J^{-1}$. See [1] for FIM derivations.

In Figure 3 we plot the CRB localization error of the sensors in Figure 2 versus the maximum principal angle ϕ_3 . This plot was generated by randomly picking 1000 locations for an anchor set of $n_a = 3$ nodes. For each anchor set location, the error and maximum principal angle were calculated and plotted. As the maximum angle approaches 90° at least one dimension becomes uninformed by either constraints or measurements and the estimation error rapidly

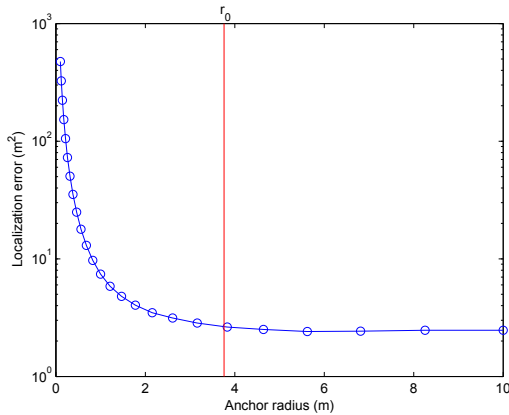


Fig. 4: Mean-square localization error of the sensors in Fig. 2 versus common anchor radius r for 3 anchor nodes uniformly spaced around a circle. The vertical bar indicates the RMS radius r_0 of the 10 unknown-location sensors.

increases. The decreasing nature of localization error with decreasing maximum principal angle ϕ_3 supports the assertion that aligning the constraint and transformation subspaces provides a viable heuristic for anchor node placement. The error is not monotonic with ϕ_3 because this single measure does not capture all of the interactions between the constraints and measurements, however minimizing the subspace angle is a good surrogate performance metric for minimizing RMS localization error.

In Figure 4 we plot CRB localization error for the sensors in Figure 2 versus a common anchor radius r for three anchors spaced equally around an r -radius circle. The point $r = r_0 = 3.76$ m is shown on the figure by the vertical bar. As expected, we see negligible performance improvement for $r > r_0$.

Finally, in Figure 5 we compare the uniform perimeter placement strategy with optimal anchor locations derived by an oracle with perfect knowledge of the sensor positions. In this example 1000 networks were generated, each consisting of 10 unknown-location sensors uniformly distributed in a circular region of radius 50 m. For each network, the oracle finds the optimal anchor positions θ_a^* of three anchors from Eq. (1). We then compare the performance of θ_a^* to perimeter-placed anchors θ_a^p (radius=50 m, 120° spacing). Let $e(\theta_a^p)$ and $e(\theta_a^*)$ denote the errors for perimeter placement and optimal placement, respectively. Using the 1000 network realizations, we plot in Figure 5 a histogram of the ratio $\gamma = e(\theta_a^p)/e(\theta_a^*)$. From the figure we see that optimal anchor placement, utilizing perfect knowledge of the sensor locations, is only marginally better than perimeter placement which only assumes sensors are constrained to a particular circular region. On average, the error of perimeter placement exceeds the error of optimal placement by only 4%.

5. CONCLUSIONS

In this paper we have demonstrated analytically that uniform perimeter placement of anchor nodes is a logical choice in the absence of any detailed information about sensor positions. This result was previously known only through limited empirical observations. We demonstrated that the relative alignment between the constraint subspace and the space of measurement-independent translations and rotations can be controlled through anchor node placement and that

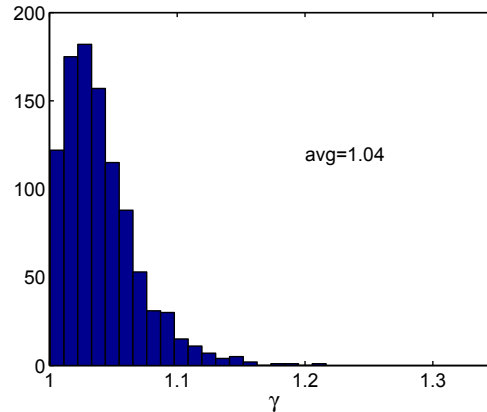


Fig. 5: Histogram of $\gamma = e(\theta_a^p)/e(\theta_a^*)$ indicating that the performance of perimeter placement is nearly as good as the oracle placement bound.

uniform perimeter placement optimally aligns these subspaces.

While the examples in this paper considered fully connected networks with distance measurements and Gaussian noise, the analytic results are more general. The uniform perimeter placement strategy, which optimally aligns the constraint and transformation subspaces, makes no assumptions about noise distributions or measurement connectivity and applies to any scenario where measurements are invariant to translation and rotation. This includes many measurement types such as distances, time-of-arrival, time-difference-of-arrival, and received-signal-strength.

6. REFERENCES

- [1] Neal Patwari, Joshua N. Ash, Spyros Kyperountas, Alfred O. Hero III, Randolph L. Moses, and Neiyer S. Correal, "Locating the nodes: cooperative localization in wireless sensor networks," *IEEE Signal Processing Magazine*, vol. 22, no. 4, pp. 54–69, July 2005.
- [2] Randolph Moses and Robert Patterson, "Self-calibration of sensor networks," *Unattended Ground Sensor Technologies and Applications IV, Proc. SPIE vol. 4743*, pp. 108–119, 2002.
- [3] Pratik Biswas, Tzu-Chen Lian, Ta-Chung Wang, and Yinyu Ye, "Semidefinite programming based algorithms for sensor network localization," *ACM Trans. on Sensor Networks*, vol. 2, no. 2, pp. 188–220, 2006.
- [4] Koen Langendoen and Niels Reijers, "Distributed localization in wireless sensor networks: a quantitative comparison," *Comput. Networks*, vol. 43, no. 4, pp. 499–518, 2003.
- [5] Andreas Savvides, Heemin Park, and Mani B. Srivastava, "The bits and flops of the n-hop multilateration primitive for node localization problems," *Intl. Workshop on Sensor Nets. & Apps.*, pp. 112–121, Sep 2002.
- [6] Joshua N. Ash and Randolph L. Moses, "Relative and absolute errors in sensor network localization," *IEEE International Conference on Acoustics, Speech, and Signal Processing*, pp. 1033–1036, April 15–20 2007.
- [7] Gene Golub and Charles Van Loan, *Matrix Computations*, Johns Hopkins University Press, 3rd edition, 1996.